Hyperecho in ultrasound images during high-intensity focused ultrasound ablation for hepatocellular carcinomas

Hiroyuki Fukuda [a],[*], Kazushi Numata [a], Akito Nozaki [a], Masaaki Kondo [a], Manabu Morimoto [a], Katsuaki Tanaka [a], Ryu Ito [b], Masao Ohto [b], Yoshiharu Ishibashi [c], Noriyoshi Oshima [c], Ayao Ito [c], Hui Zhu [d], Zhi-Biao Wang [e]

[a] Gastroenterological Center, Yokohama City University Medical Center, 4-57 Urafune-cho, Minami-ku, Yokohama, Kanagawa 232-0024, Japan
[b] International HIFU Center, Sanmu Medical Center Hospital, Naruto167, Sanmu-shi, Chiba 289-1326, Japan
[c] Clinical Development Group, AVS, 1-22-2 Nishishinjuku, Tokyo 160-0023, Japan
[d] Clinical Center of Tumor Therapy of 2nd Affiliated Hospital, Chongqing University of Medical Sciences, Chongqing, China
[e] Institute of Ultrasonic Engineering in Medicine, Chongqing University of Medical Sciences, Chongqing, China

ARTICLE INFO

ABSTRACT

High-intensity focused ultrasound (HIFU) is a noninvasive method that can cause complete coagulation necrosis without requiring the insertion of any instruments. The hyperechoic grayscale change (hyperechoic region) is used as a sign that the treated lesion has been completely coagulated. The purpose of this study was to evaluate the first hyperechoic region during treatment using HIFU ablation according to various conditions, such as the sonication power, the depth of the tumor from the surface of the skin, and the shield rate. HIFU treatment was performed in 20 patients. The HIFU system (Chongqing Haifu Tech, Chongqing, China) was used under ultrasound guidance. Complete coagulation was achieved in 17 cases. Hyperechoic region were detected after HIFU ablation in 17 patients. The size of the hyperechoic region at a depth of >50 mm was significantly smaller than that at a depth of ≤50 mm. The number and power of the sonications for areas at a depth of >50 mm were significantly larger than those for areas at a depth of ≤50 mm. The number and power in cases with a shield rate of 31–60% were significantly larger than those in cases with a shield rate of 0–30%. When the shield rate was 0%, a hyperechoic region occurred, even when a maximum sonication power was not used. In all three cases with tumors located at a depth of greater than 70 mm and a shield rate of larger than 60%, a hyperechoic region was not seen. In conclusion, hyperechoic regions are easy to visualize in cases with tumors located at a depth of ≤50 mm or shield rates of 0–30%.

1. Introduction

High-intensity focused ultrasound (HIFU), a noninvasive method that can cause complete coagulation necrosis without requiring the insertion of any instruments [1–5], has been applied for the treatment of several human neoplasms [6], including the treatment of small hepatocellular carcinoma (HCC) [7,8].

The ultrasound (US)-guided HIFU therapy system used in the present study was unable to monitor the temperature in the ablated area. To compensate for this limitation, a change in the hyperechoic grayscale (hyperechoic region) was used as a sign that the treated lesion had been completely coagulated [9]. Some previous reports have evaluated hyperechoic region and tissue necrosis [10,11]. A hyperechoic region is considered to indicate tissue necrosis and has been used to judge complete ablation [12].

Wu et al. [13] performed a rib resection to provide an adequate acoustic window for the treatment of large HCCs (mean, 10.3 cm). Zhu et al. [4] also performed a partial rib resection to create a better acoustic pathway for HIFU therapy. Wang et al. [9] evaluated the relationship between the volume of the ablation and the depth using bovine liver tissue. However, no previous report has evaluated the relationship between the volume of the ablation and the depth, sonication power, and shield rate produced by the ribs and lung gas in clinical liver tissues. The purpose of the present study was to evaluate the hyperechoic region observed first during HIFU treatment according to various conditions, such as the sonication power, the depth from the surface of the skin, and the shield rate.

2. Materials and methods

2.1. Patients

Between July 2007 and October 2008, 20 patients with HCC were enrolled in this clinical study. These 11 men and 9 women ranged

* Corresponding author. Tel.: +81 45 261 5656; fax: +81 45 261 9492.
E-mail address: fukuhiro1962@hotmail.com (H. Fukuda).

in age from 65 to 80 years old (mean, 73.6 years). The maximum diameter of the tumors measured using sonography ranged from 10 to 19 mm (mean, 15.4 mm; SD, 2.8 mm). The patients had Child-Pugh classification A or B liver cirrhosis, a prothrombin time ratio greater than 50%, and a platelet count greater than 50,000 mm^{-3}. In two patients, the diagnosis of hepatocellular carcinoma was confirmed using a percutaneous needle biopsy. The remaining 18 patients were diagnosed as having hepatocellular carcinoma based on the imaging findings (newly presenting tumor on follow-up ultrasonography in patients with chronic liver disease and characteristic enhancement pattern on contrast-enhanced, multiphase helical computed tomography [CT] or contrast-enhanced magnetic resonance imaging [MRI]). All 20 patients had liver cirrhosis as a result of hepatitis C. At the time of HIFU, the patients were classified as having Child-Pugh classifications A ($n = 16$) or B ($n = 4$) cirrhosis. Transarterial chemoembolization (TACE), percutaneous ethanol injection (PEI) and rib resection were not performed prior to HIFU treatment. Prior to treatment, each patient's skin was shaved and degassed using a suction pump. An epidural anesthesia was used during the procedure. Our hospital ethics committee approved this study, and each patient signed an informed consent form at the time of enrollment.

2.2. Ultrasound therapy system

Sonications were performed using a clinical US guided ultrasound surgery system. The Tumor Therapy System (Model AC 0501; Chongqing Haifu Tech Co., Ltd., Chongqing, China) used in this study was guided using real-time ultrasonographic imaging [14]. An HIFU 6150S US imaging unit was installed on the HIFU system to enable real-time US imaging during HIFU ablation. A 2–5 MHz imaging probe was located at the center of the HIFU transducer and was mounted in a reservoir of degassed water [13]. Therapeutic US energy was produced using a piezoelectric ceramic transducer with a diameter of 20 cm, a focus length of 15 cm and an operating frequency of 1.0 MHz. The focal lesion was ellipsoid, with dimensions of 9.8 mm along the beam axis and 1.3 mm in the transverse direction. The targeted tissue was exposed to acoustic focal peak intensities of 5000 and 15,000 W/cm^2. A calibrated polyvinylidene difluoride membrane hydrophone with a spot diameter of 0.5 mm (Shanghai Jiao Tong University, Shanghai, China) was used to map the acoustic pressure field of the focused transducer at peak intensities of from 200 to 300 W/cm^2. After the induction of suitable anesthesia, the patient was carefully positioned either prone or on his or her right side so that the skin overlying the lesion to be treated could be easily placed in contact with the degassed water. We checked for pain or complications and then gradually increased the ultrasound power up to 240–450 W. The time period for one sonication was 5 s. During the focused ultrasound ablation of each section, the real-time US images obtained before and after each exposure were immediately compared to determine whether the hyperechoic region, indicating the extent of coagulation necrosis, had covered the desired treatment area [10,15]. Patients were trained to hold their breath at the point at which their entire tumor became visible when the tumor was located between the ribs or just behind the diaphragm.

2.3. Calculation of shield rate, depth and size of the hyperechoic region

The shield rate of the rib shadow and the lung shadow was calculated using US monitoring when a hyperechoic region was observed. The shield rate of the rib shadow and lung shadow was calculated as the ratio of the rib shadow and lung shadow to the HIFU projection at the body surface. The depth of the hyperechoic region was measured as the length between the center of the

hyperechoic region and the skin surface. The size of the hyperechoic region was calculated as the longitudinal length. The power and accumulated number of sonications at the point where the hyperechoic region was observed were evaluated in this clinical study. In this study, the total accumulated number of sonications was evaluated even for cases in which a hyperechoic region was not seen; in these cases, the size of the hyperechoic region was regarded as 0 mm in diameter. In case where a hyperechoic region was not observed, the shield rate of the rib shadow and lung shadow was calculated using US monitoring at the point where the focus of the HIFU was located at the center of the tumor.

2.4. Assessment of treatment efficacy and follow-up

Dynamic CT scans (Aquilion TSX-101A; Toshiba Medical Systems Corp., Tokyo, Japan) with a section thickness of 5 mm were obtained to evaluate the ablation. Complete ablation according to a CT scan was defined as the hypoattenuated area, including the surrounding liver parenchyma, at 1 week after the HIFU procedure [16].

Dynamic MRI scans (Signa HDX 3.0 T system; GE Healthcare, Milwaukee, WI) with gradient-echo (GRE) sequences and T1 fat saturation (TR/TE, 4.8/1.9; flip angle, 12°; matrix size, 320 × 192; section thickness, 4 mm; intersection gap, 0–2 mm; one acquisition) were performed. The scan delay times were 22 s, 60 s and 30 min after the bolus injection of a 0.025 mmol dose of gadolinium-ethoxybenzyl-diethylenetriamine pentaacetic acid (d-EOB-DTPA) (Primovist; Bayer Schering Pharma)/kg body weight. Assessment using dynamic MRI scans were performed when the tumors were not detected by dynamic CT scans.

Assessments using contrast-enhanced (0.2 mL of Sonazoid suspension; Daiichi Sankyo, Tokyo, Japan) ultrasonography (LOGIQ 7; GE Healthcare, Milwaukee) were performed in all the patients when the hyperechoic region covered the original tumor and at 1 week after the HIFU procedure. A convex volume 4D3C-L probe (GE Healthcare) was used. All the patients received an intravenous bolus injection of 0.2 mL of Sonazoid via a 24-gauge cannula into a forearm vein, followed by 2 mL of a 5% glucose solution and the subsequent infusion of a 5% glucose solution at 10 mL/min. A coded harmonic angio (CHA) mode with a high mechanical index (0.5–0.9) at 8–13 frames per second was selected for the contrast-enhanced, three-dimensional US procedure. The focus point was set beneath the tumor [5]. Complete ablation based on the contrast-enhanced ultrasonography findings was defined as a perfusion defect with no enhancement and no tumor vessels during both the early vascular phase and the post vascular phase [17].

2.5. Statistical analysis

All the data were reported as the mean ± standard deviation. The difference between the sonication times according to the size, number and power of the hyperechoic region were evaluated using the Mann–Whitney U-test. Statistical significance was defined as a p value of less than 0.05.

3. Results

Hyperechoic regions were detected after HIFU ablation in 17 patients (Figs. 1a, b and 2a, b). Table 1 shows the size of the hyperechoic region, the number of sonications, and the HIFU exposure power at the time of the initial appearance of a hyperechoic region according to patient posture, the depth from the surface of the skin, and the shield rate.

Treatment was achieved by sonication from the right intercostal space when the tumor was located in the right lobe ($n = 10$) and while the patient was in a prone position when the tumor was
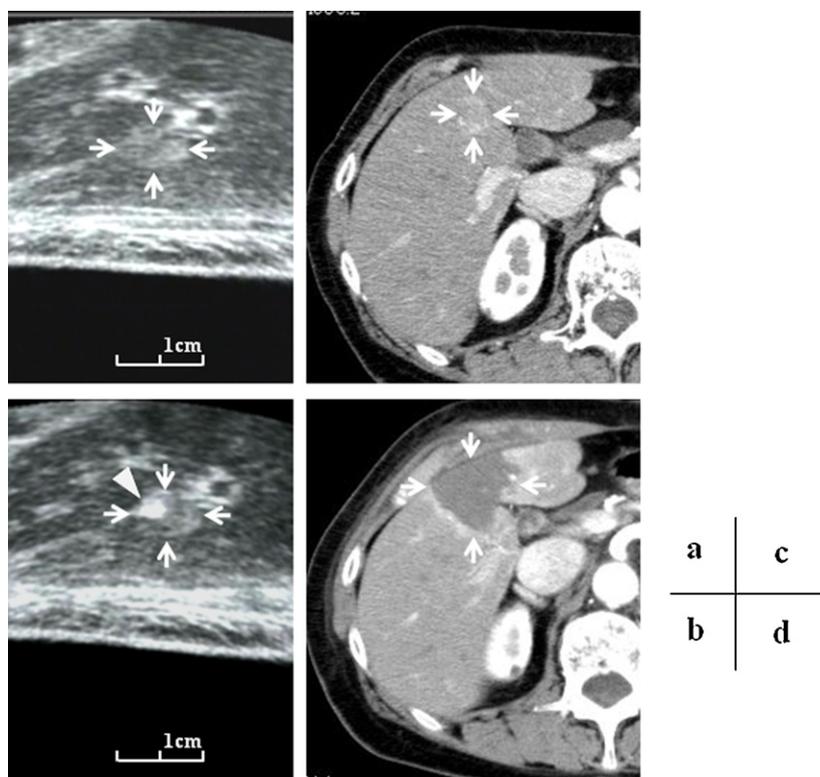
Fig. 1. (a) US image obtained before the HIFU treatment shows a hyperechoic tumor 15 mm × 12 mm in size (arrow). (b) A hyperechoic region (arrow head) was detected after 2 HIFU sonications at a power of 240 W and depth of 35 mm from the surface of the skin. The shield rate in this case was 0%. The diameter of the hyperechoic region was 5 mm (arrow head). (c) A CT scan obtained before the HIFU treatment shows a hyperattenuated area with a diameter of 15 mm during the arterial phase (c) (arrow) and low attenuation during the equilibrium phase. A CT scan obtained 7 days after HIFU treatment shows a 40 mm × 38 mm necrotic area (d) (arrow), which was large enough to encompass the safety margin. The decreased vascular flow implied tissue devascularization and necrosis, suggesting that the region had been treated effectively.

located in the left lobe ($n = 10$). No statistical difference in the sizes of the initial hyperechoic regions was seen when this parameter was compared according to the prone and right lateral positions. Furthermore, when the prone and right lateral positions were compared, no differences in the number or power of the sonications at the time of the observation of the initial hyperechoic regions were seen.

Regarding the relationship between the tumor depth and the hyperechoic region (Table 1), the size of the hyperechoic region at a tumor depth > 50 mm was significantly smaller than that at a tumor depth ≤50 mm ($p < 0.05$). The number and the power of the sonications at the time when the hyperechoic regions first emerged for tumors at a depth of >50 mm was significantly larger than that for hyperechoic regions for tumors a depth of ≤50 mm ($p < 0.05$, $p < 0.01$).

Regarding the relationship between the shield rate and the hyperechoic region (Table 1), the size of the hyperechoic region in cases with a shield rate of 0–30% was larger than that in cases with a shield rate of 31–60%, although the difference was not significant. The number and power of sonications in cases with a shield rate of 31–60% was significantly larger than that in cases with a shield rate of 0–30% ($p < 0.01$).

In three cases with a tumor depth greater than 70 mm and a shield rate of larger than 60%, hyperechoic regions were not observed. The treatments in 2 of these 3 cases were regarded as effective based on evaluations of the CT findings obtained after HIFU treatment, but tumor residue was observed after the treatment of the third case.

Complete coagulation was achieved in 17 cases, while the coagulation was incomplete in 3 cases. A hyperechoic region was not

Table 1
Size of hyperechoic region, number of sonications, and high-intensity focused ultrasound (HIFU) exposure power at the time when the first hyperechoic region emerged according to posture, the depth from the surface of the skin and the shield rate.

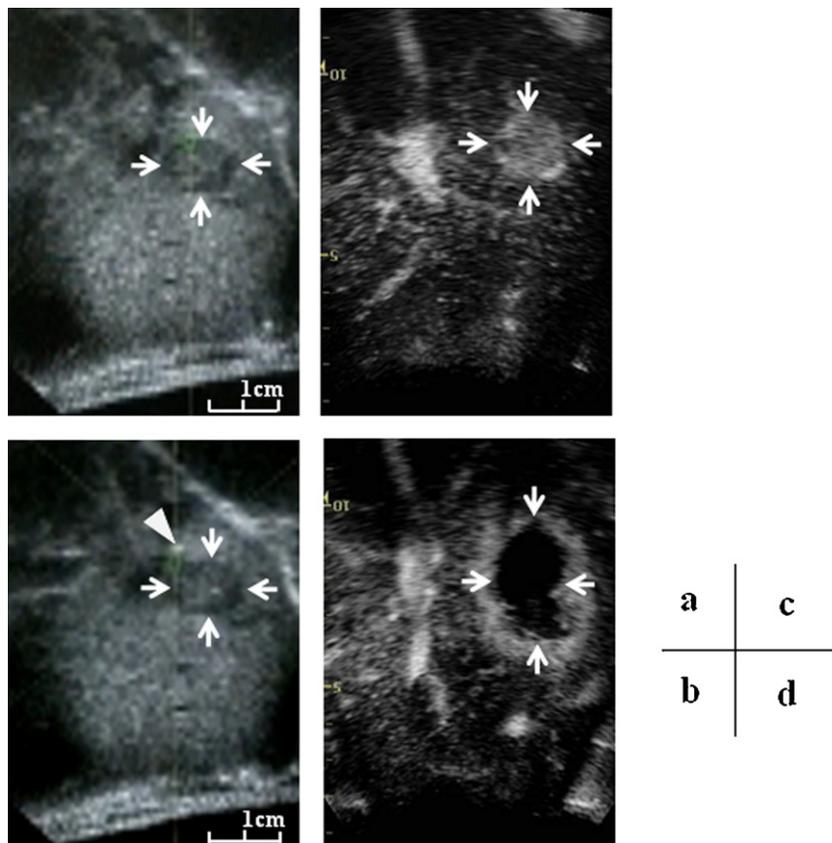|	Size (mm) of hyperechoic region	Number of sonications	HIFU exposure power (W)
Posture			
Prone ($n = 10$)	1.9 ± 1.8	41.5 ± 60.8	329 ± 95.9
Right lateral ($n = 10$)	3.0 ± 2.6	38.4 ± 53.4	403 ± 87.3
	NS	NS	NS
Depth			
≤50 mm ($n = 6$)	4.2 ± 2.6	4.5 ± 2.8	270 ± 32.9
>50 mm ($n = 14$)	1.7 ± 1.6	55.1 ± 60.8	407 ± 85.2
	$p < 0.05$	$p < 0.05$	$p < 0.01$
Shield rate			
0–30% ($n = 12$)	2.83 ± 2.3	10.4 ± 16.4	310 ± 87.7
31–60% ($n = 8$)	1.88 ± 2.1	84.3 ± 65.2	450 ± 0
	NS	$p < 0.01$	$p < 0.01$

Fig. 2. (a) US image obtained before the HIFU treatment shows a hypochoic tumor with a diameter of 20 mm (arrow). (b) A hyperechoic region (arrow head) was detected after 11 HIFU sonications at a power of 450 W and a depth of 84 mm from the surface of the skin. The shield rate in this case was 35%. The diameter of the hyperechoic region was 2 mm (arrow head). Contrast enhanced US image obtained before (arrow) (c) and just after HIFU treatment (arrow) (d). The blood flow disappeared after HIFU.

observed in one of these 3 incomplete cases. On the other hand, hyperechoic regions were observed in 2 of the 3 incomplete cases.

4. Discussion

In the US-guided HIFU therapy system used in the present study, a change in the hyperechoic grayscale (hyperechoic region) was regarded as a sign that the treated lesion had been completely coagulated, since the system itself was unable to perform thermometry of the ablated area [9,13,15]. The hyperechoic region representing the HIFU treatment site results from bubble activity generated during HIFU exposure [13,15]. The presence of cavitation in the US field was also correlated with a rapid rise in temperature both in vitro [18] and in vivo [19,20]. Wang et al. [9] evaluated the relationship between the volume of the ablation and the depth in bovine liver tissue and concluded that the volume of the ablation decreased as the irradiation depth within the tissue increased. However, the relationships between the hyperechoic region at the HIFU treatment site and several conditions, such as the tumor depth, power of sonication, and shield rate, in clinical liver studies have not been previously evaluated.

The percentage of trials in which a hyperechoic region was visualized reportedly increased as the average HIFU intensity increased [10]. In this study, the power necessary to produce a hyperechoic region for an area at a depth of >50 mm was significantly larger than that for an area at a depth of ≤50 mm because of the attenuation according to the depth. Furthermore, the power required to produce a hyperechoic region in cases with a shield rate of 31–60% was significantly larger than that for cases with a shield rate of 0–30%. When the shield rate was 60%, it was difficult to detect a hyperechoic region even if a maximum sonication power was applied. Furthermore, the appearance of a hyperechoic region on US image reportedly correlates with the HIFU intensity increases during both active and passive cavitation detection [10]. The average HIFU exposure time needed to visualize a hyperechoic region and to detect cavitation was inversely related to the in situ HIFU intensities [10]. In the present study, the number of sonications required to produce a hyperechoic region in an area at a depth of >50 mm was significantly larger than that for an area at a depth of ≤50 mm. The number of sonications in cases with a shield rate of 31–60% was significantly larger than that in cases with a shield rate of 0–30%. Wang et al. [9] evaluated the relationship between the volume of the ablation and the depth in bovine liver tissue and concluded that the volume of the ablation decreased as the irradiation depths within the tissue increased. In the present study, the size of the hyperechoic region for areas at a depth of >50 mm was significantly smaller than that for areas at a depth of ≤50 mm.

Wu et al. [14] reported that a portion of the ribs was resected to provide an adequate acoustic window because the average size of the HCCs in their study was relatively large (mean, 10.3 cm). And Zhu et al. [4] evaluated the efficacy and safety of HIFU treatment after a partial rib resection and concluded that a partial rib resection can create a better acoustic pathway for HIFU therapy. They emphasized that a partial rib resection improved the prospect of complete tumor ablation when no other treatment was available, even though such resections are invasive. We think that their rib resection protocol was effective because their average tumor size was 7 cm in diameter, but we did not perform a rib resection because the average tumor size in our study was less than 2 cm. When the shield rate was 0%, a hyperechoic region was easily produced even at a relatively low sonication power. On the other hand, when the shield rate was 60%, a hyperechoic region was difficult

to detect and the size of the detected lesions was relatively small (1 mm in diameter).

In this study, complete coagulations were achieved in 17 cases, and 3 cases with tumor residue were observed. Two of the 3 cases with tumor residue were thought to have been difficult cases because of the depth of the tumors and the relatively high shield rates (Case1: tumor depth of 85 mm and shield rate of 40%, Case 2: tumor depth of 80 mm and shield rate of 60%). The reason for the tumor residue in the third case (Case 3: tumor depth of 65 mm and shield rate of 30%) was thought to be that the safety margin for this tumor was insufficient, although a hyperechoic region was clearly detected after the third sonication.

Generally, tumors located in the left lobe are regarded as being easy to ablate because the shield rate for these tumors is typically low. However, it was not easy to make hyperechoic region even if the tumor was located in the left lobe in this study (Table 1), and the depth of the tumor and the shield rate had to be kept in mind. Hyperechoic regions were more difficult to produce in cases where the tumor was located in the upper portion of the left lobe, i.e., in areas where the ribs tended to shield the tumor from the sonications. On the other hand, hyperechoic regions were easily produced when the tumor was located near the surface of the liver, even when the tumor was located in the right lobe.

The treatments in 2 of the 3 cases where a hyperechoic region was not produced were, nevertheless, regarded as effective, while tumor residue was observed in the third case. Thus, the emergence of a hyperechoic region is not an absolute sign that the HIFU treatment has been completed. A contrast-enhanced US examination may be necessary in cases where a hyperechoic region is not observed.

In conclusion, hyperechoic regions are easy to produce in cases with a tumor located at a depth of ≤50 mm or a shield rate of 0–30%.

References

[1] ter Haar G. High intensity ultrasound. Semin Laparosc Surg 2001;8:77–89.
[2] Hynynen K, Pomeroy O, Smith DN, et al. MR imaging-guided focused ultrasound surgery of fibroadenoma in the breast: a feasibility study. Radiology 2001;219:176–85.
[3] Jolesz FA, Hynynen K, McDannold N, Freundlich D, Kopelman D. Noninvasive thermal ablation of hepatocellular carcinoma by using magnetic resonance imaging-guided focused ultrasound. Gastroenterology 2004;127:S242–7.
[4] Zhu H, Zhou K, Zhang L, et al. High intensity focused ultrasound (HIFU) therapy for local treatment of hepatocellular carcinoma: role of partial rib resection. Eur J Radiol 2009;72:160–6.
[5] Numata K, Fukuda H, Ohto M, et al. Evaluation of the therapeutic efficacy of high-intensity focused ultrasound ablation of hepatocellular carcinoma by three-dimensional sonography with a perflubutane-based contrast agent. Eur J Radiol 2010;75:e67–75.
[6] Tempany CM, Stewart EA, McDannold N, et al. MR image-guided focused ultrasound surgery of uterine leiomyomas: a feasibility study. Radiology 2003;226:897–905.
[7] Fukuda H, Numata K, Nozaki A, et al. Usefulness of US-CT 3D dual imaging for the planning and monitoring of hepatocellular carcinoma treatment using HIFU. Eur J Radiol, in press.
[8] Fukuda H, Numata K, Nozaki A, et al. Findings of multidetector row computed tomography of HCCs treated by HIFU ablation. Eur J Radiol, in press.
[9] Wang Z, Bai J, Li F, et al. Study of a 'biological focal region' of high-intensity focused ultrasound. Ultrasound Med Biol 2003;29:749–54.
[10] Rabkin BA, Zderic V, Vaezy S. Hyperecho in ultrasound images of HIFU therapy: involvement of cavitation. Ultrasound Med Biol 2005;31:947–56.
[11] Rabkin BA, Zderic V, Crum LA, Vaezy S. Biological and physical mechanisms of HIFU-induced hyperecho in ultrasound images. Ultrasound Med Biol 2006;32:1721–9.
[12] Coussios CC, Farny CH, Haar GT, Roy RA. Role of acoustic cavitation in the delivery and monitoring of cancer treatment by high-intensity focused ultrasound (HIFU). Int J Hyperther 2007;23:105–20.
[13] Wu F, Wang ZB, Chen WZ, et al. Extracorporeal high intensity focused ultrasound ablation in the treatment of patients with large hepatocellular carcinoma. Ann Surg Oncol 2004;11:1061–9.
[14] Wu F, Wang ZB, Cao YD, et al. A randomised clinical trial of high-intensity focused ultrasound ablation for the treatment of patients with localised breast cancer. Br J Cancer 2003;89:2227–33.
[15] Vaezy S, Shi X, Martin RW, et al. Real-time visualization of high-intensity focused ultrasound treatment using ultrasound imaging. Ultrasound Med Biol 2001;27:33–42.
[16] Ebara M, Okabe S, Kita K, et al. Percutaneous ethanol injection for small hepatocellular carcinoma: therapeutic efficacy based on 20-year observation. J Hepatol 2005;43:458–64.
[17] Hotta N, Tagaya T, Maeno T, et al. Advanced dynamic flow imaging with contrast-enhanced ultrasonography for the evaluation of tumor vascularity in liver tumors. Clin Imaging 2005;29:34–41.
[18] Holt RG, Roy RA. Measurements of bubble-enhanced heating from focused, MHz-frequency ultrasound in a tissue-mimicking material. Ultrasound Med Biol 2001;27:1399–412.
[19] Hynynen K. The threshold for thermally significant cavitation in dog's thigh muscle in vivo. Ultrasound Med Biol 1991;17:157–69.
[20] Sokka SD, King R, Hynynen K. MRI-guided gas bubble enhanced ultrasound heating in in vivo rabbit thigh. Phys Med Biol 2003;48:223–41.